

**LIGHT SCATTERING, ATOMIC FORCE MICROSCOPY AND FLUORESCENCE CORRELATION SPECTROSCOPY STUDIES OF POLYSTYRENE-*block*-POLY(2-VINYLPYRIDINE)-*block*-POLY(ETHYLENE OXIDE) MICELLES<sup>+</sup>**

Miroslav ŠTĚPÁNEK<sup>a1</sup>, Jana HUMPOLÍČKOVÁ<sup>a2</sup>, Karel PROCHÁZKA<sup>a3,\*</sup>, Martin HOF<sup>b</sup>, Zdeněk TUZAR<sup>c1</sup>, Milena ŠPÍRKOVÁ<sup>c2</sup> and Thomas WOLFF<sup>d</sup>

<sup>a</sup> *Department of Physical and Macromolecular Chemistry and Laboratory of Specialty Polymers, Faculty of Science, Charles University, Albertov 6, 128 43 Prague 2, Czech Republic;*

*e-mail:* <sup>1</sup> [stepanek@prfdec.natur.cuni.cz](mailto:stepanek@prfdec.natur.cuni.cz), <sup>2</sup> [humpolic@natur.cuni.cz](mailto:humpolic@natur.cuni.cz),

<sup>3</sup> [prochaz@vivien.natur.cuni.cz](mailto:prochaz@vivien.natur.cuni.cz)

<sup>b</sup> *J. Heyrovský Institute of Physical Chemistry, Academy of Sciences of the Czech Republic and Center for Complex Molecular Systems and Biomacromolecules, Dolejškova 3, 182 23 Prague 8, Czech Republic; e-mail:* [hof@jh-inst.cas.cz](mailto:hof@jh-inst.cas.cz)

<sup>c</sup> *Institute of Macromolecular Chemistry, Academy of Sciences of the Czech Republic, Heyrovského nám. 2, 162 06 Prague 6, Czech Republic; e-mail:* <sup>1</sup> [tuzar@imc.cas.cz](mailto:tuzar@imc.cas.cz),

<sup>2</sup> [spirkova@imc.cas.cz](mailto:spirkova@imc.cas.cz)

<sup>d</sup> *Institute of Physical Chemistry and Electrochemistry, Dresden Technical University, Mommsenstrasse 13, 01062 Dresden, Germany; e-mail:* [thomas.wolff@chemie.tu-dresden.de](mailto:thomas.wolff@chemie.tu-dresden.de)

Received April 10, 2003

Accepted June 13, 2003

Polymeric nanoparticles formed by triblock copolymer polystyrene-*block*-poly(2-vinylpyridine)-*block*-poly(ethylene oxide), PS-PVP-PEO, in aqueous media were studied by a combination of fluorescence correlation spectroscopy with other fluorescence techniques, light scattering and atomic force microscopy. The studied polymeric nanoparticles exist in the form of (i) core/shell micelles in acid solution at pH lower than 4.8 and (ii) three-layer on-ion micelles at higher pH. Since water is a very strong precipitant for PS, both types of micelles have kinetically frozen spherical PS cores. The cores of micelles in acid media are surrounded by soluble shells formed by partly protonated PVP and PEO, while the cores of micelles in alkaline media are surrounded by compact insoluble layers of deprotonated PVP and soluble PEO shells. The micellization behavior of PS-PVP-PEO micelles is accompanied by secondary aggregation of micelles, which is provoked by stirring, shaking and also by filtration of micellar solutions. Therefore fluorescence correlation spectroscopy (FCS), which, in contrast to light scattering techniques, does not require filtration, was used as the main experimental technique for the characterization of non-aggregated micelles. The binding of

+ The study is a part of a Long-Time Research Plan of the Faculty of Science of the Charles University, MSM 1131 00001.

a fluorescence probe, octadecylrhodamine B (ORB), to polymeric micelles, was studied before the FCS study of micelles.

**Keywords:** Block copolymer micelles; Onion micelles; Water-soluble polymers; Polystyrene; Poly(2-vinylpyridine); Poly(ethylene oxide); Octadecylrhodamine B; Light scattering; Fluorescence; Fluorescence correlation spectroscopy; Atomic force microscopy.

Amphiphilic block polyelectrolyte micelles are interesting nanoparticles, which offer a number of potential applications in various fields. They do not usually form spontaneously upon dissolution since the high-molecular-weight block copolymers with long hydrophobic blocks are insoluble in aqueous media, but they can be prepared indirectly, *e.g.*, by dialysis. Thanks to the practical importance of various micelle-based nanoparticles, the micellization of water-soluble polymers has been the subject of numerous studies. The number of pertinent studies is so vast that it is futile to give all relevant references. Therefore we mention only the relatively recent books by Webber, Tuzar and Munk<sup>1</sup> and by Hamley<sup>2</sup> and the references therein. We have been studying the micellization of block copolymer micelles in aqueous and other selective media by a combination of several experimental techniques<sup>3</sup> and theoretically (by Monte Carlo simulations<sup>4</sup>) for more than one decade.

In this work, we present the first part of results concerning the micellization of polystyrene-*block*-poly(2-vinylpyridine)-*block*-poly(ethylene oxide), PS-PVP-PEO, in aqueous solutions. The micellization behavior of this copolymer is very interesting. Polystyrene (PS) is insoluble in aqueous media and forms micellar cores. Poly(ethylene oxide) (PEO), a water-soluble polymer, forms the micellar shell. Poly(2-vinylpyridine) (PVP) is protonated and soluble in acid solutions at pH lower than 4.8, while the deprotonated PVP that exists at higher pH is water-insoluble. In the systems studied, we expect that PVP chains form a middle layer of three-layer micelles. The middle layer should be either collapsed at high pH or partly protonated, swollen and relatively flexible in acid media. In the latter case, it may be partly mixed with PEO. Some time ago, we reported the preparation of onion-type micelles in mixtures of poly(*tert*-butyl acrylate)-*block*-poly(2-vinylpyridine) micelles (PBA-PVPH<sup>+</sup>) with poly(2-vinylpyridine)-*block*-poly(ethylene oxide) dissolved as single PVPH<sup>+</sup>-PEO chains at low pH<sup>3e</sup>. The mixed three-layer micelles were formed as a result of the coprecipitation of poly(2-vinylpyridine) blocks of PBA-PVP and PVP-PEO in the alkalimetric titration of acid aqueous mixtures at pH close to 4.8.

With respect to the above-mentioned study, the micellization behavior of PS-PVP-PEO copolymers is expected to be simple as compared with the formation of mixed micelles. The transition from state I (micelles with insoluble PS cores and soluble shells formed by partly protonated PVP and PEO at low pH) to state II (onion micelles with PS cores covered by a collapsed deprotonated PVP middle layer and PEO shells at high pH) seems to be an obvious and absolutely natural process. To our surprise, the micellization behavior of the studied copolymers is quite complex. The micelles are apt to aggregate, probably due to the fairly reduced solubility of highly concentrated PEO chains in micellar shells<sup>5</sup>. The aims of the present paper are: (i) to design suitable recipes for the preparation of onion micelles and to test their reproducibility, (ii) to characterize the prepared micelles and (iii) to study the pH-induced transition and properties of both types of micelles and (iv) to find efficient ways to prevent or at least suppress secondary aggregation of micelles.

Since the formation of micellar aggregates is provoked mainly by stirring, shaking or even by a mild pressure filtration of the solution through the Acrodisc filters, we use the fluorescence correlation spectroscopy<sup>6</sup> as the main technique for the characterization of micelles. This relatively new technique is nowadays quite popular in biochemistry and molecular biology<sup>7</sup>, but it has been only little used in polymer chemistry<sup>8</sup>. Therefore it is interesting to test its potential and its limitations in polymer research. This technique yields the number-average molar mass  $M_n$  and the "number-average" hydrodynamic radius  $R_H$  of micelles (more precisely  $R_H$  based on the number-average diffusion coefficient). Its main advantages are (i) negligible consumption of samples, (ii) the possibility to measure non-filtered solutions and (iii) the possibility to study one fluorescent species in a mixture with many other non-fluorescent polymeric particles. In our particular case, the main disadvantage is the necessity of labeling the micelles with a suitable fluorescent probe. In the present and accompanying papers, we would like to demonstrate that octadecylrhodamine B (ORB) is an excellent probe for labeling polymeric micelles in aqueous media. If spectroscopic properties of the water-dissolved and micelle-bound ORB are known and well understood, the labeling does not cause any problems and the study of ORB-labeled micelles by fluorescence correlation spectroscopy (FCS) is easy and provides reliable experimental data.

## EXPERIMENTAL

## Materials

*Octadecylrhodamine B* was purchased from Molecular Probes, U.S.A.

*Solvents.* 1,4-Dioxane and methanol were purchased from Aldrich, U.S.A., and used without other purification. Deionized water was used in the study.

*Block copolymers.* Two triblock copolymers of polystyrene-*block*-poly(2-vinylpyridine)-*block*-poly(ethylene oxide) with a narrow distribution of molar masses and compositions were purchased from Polymer Source, Inc., Canada, and used as obtained. Molar masses and polydispersity of the copolymers (data provided by the producer) are summarized in Table I. Copolymer II was used for the systematic study. Copolymer I was used only for a few supplementary measurements.

*Preparation of micelles.* Since the copolymers used are not soluble in aqueous media, polymeric micelles were prepared indirectly by a combination of titration and dialysis<sup>3e</sup>. Two types of micelles were prepared for further studies:

a) Core/shell micelles in acid aqueous solutions were prepared as follows. The copolymer was dissolved in a 1,4-dioxane-methanol mixture (80 vol.%) and slowly titrated with methanol under very mild stirring until the 50% methanol content was reached. Then the solution was carefully titrated with 0.01 M HCl aqueous solution until 50% water content was reached. During the titration a typical bluish opalescence appeared due to strong light scattering from micelles. The final step consisted in the dialysis of the solution against 0.01 M HCl. During the dialysis, the HCl solution in the external bath was exchanged several times to assure complete removal of organic solvents. In this way, micelles with compact PS cores and protective shells formed by the inner layer of partly protonated PVP and the peripheral layer of PEO were prepared.

b) Onion micelles with compact PS cores surrounded by the collapsed middle layer formed by deprotonated PVP blocks and stabilized by soluble PEO shells were prepared by two different methods: (i) by dialysis similarly to micelles in aqueous media, except that either pure water or 0.01 M aqueous NaOH were added instead of 0.01 M aqueous HCl, (ii) the core/shell micelles prepared in aqueous media were converted to onion micelles by alkalimetric titration or by dialysis against 0.01 M NaOH.

A modification of the latter method was used to convert onion micelles prepared in 0.01 M NaOH to core/shell micelles by dialysis against 0.01 M HCl.

TABLE I

Characteristics of the used PS-PVP-PEO copolymers: molar masses,  $M_n$ , of the blocks and polydispersity index,  $M_w/M_n$

PS-PVP-PEO	$M_n \times 10^{-3}$ , g mol <sup>-1</sup>			$M_w/M_n$
	PS	PVP	PEO	
Copolymer I	20.1	14.2	26.0	1.10
Copolymer II	14.1	12.3	35.0	1.08

## Techniques

**Fluorescence correlation spectroscopy.** All measurements were performed with a binocular microscope ConfoCor I, Carl Zeiss, Germany, equipped with a 514 nm argon laser, an adjustable pinhole together with a special fluorescence optics, SPCM-200PQ detection diode and an ALV-5000 correlator (ALV Langen, Germany). FCS is a technique in which temporal fluctuations in the fluorescence measured from a sample of fluorescent substances are analyzed to obtain information about processes that give rise to fluorescence fluctuations. In this work we focus only on the translational diffusion and photobleaching due to the intersystem crossing as a complicating process. Time-fluctuating fluorescence intensity measured from a small irradiated volume,  $F(t)$ , is given by the following formula<sup>9</sup>

$$F(t) = \kappa Q \int W(\mathbf{r}, t) C(\mathbf{r}, t) dV, \quad (1)$$

where  $\kappa$  is the proportionality constant,  $Q$  is the product of absorptivity, fluorescence quantum yield and experimental collection efficiency,  $C(\mathbf{r}, t)$  is the concentration of fluorescent species at position  $\mathbf{r}$  in time  $t$  and  $W(\mathbf{r}, t)$  is a product of intensity profile of the incident laser beam (usually assumed to be a Gaussian profile) and functions that characterize the irradiated volume. The normalized autocorrelation function of fluctuations, which is used for the evaluation of the diffusion coefficients is given by the following generic equation

$$G(\tau) = 1 + \langle F(t)F(t + \tau) \rangle / \langle F(t) \rangle^2, \quad (2)$$

where  $F(t)$  is the fluorescence intensity in time  $t$  and  $F(t + \tau)$  is the intensity in time  $(t + \tau)$  and the averaging is performed over the whole measured time interval. Several models differing in complexity have been treated theoretically<sup>10</sup>. According to experimental conditions, a roughly cylindrical volume of the radius  $\omega_1$  and height  $2\omega_2$  irradiated with a focused laser beam with Gaussian intensity profile is usually considered. If this volume contains two types of fluorescent particles with quantum yields and absorptivities  $q_1$ ,  $q_2$  and  $A_1$ ,  $A_2$ , respectively, and the same probability of the intersystem crossing (e.g., one probe distributed in two different microenvironments), the function  $G(\tau)$  assumes the following form<sup>10a,10b</sup>

$$G(\tau) = 1 + \frac{1}{N(1-T)} \left\{ 1 - T(1 - e^{-\tau/\tau_0}) \right\} \times \left\{ \frac{1-Y}{1 + (\tau/\tau_1)} \frac{(A_1 q_1)^2}{[1 + S^2(\tau/\tau_1)]^{1/2}} + \frac{Y}{1 + (\tau/\tau_2)} \frac{(A_2 q_2)^2}{[1 + S^2(\tau/\tau_2)]^{1/2}} \right\}, \quad (3)$$

where  $N$  is the particle number (i.e., total number of fluorescent particles in this volume),  $Y$  and  $(1 - Y)$  are mole fractions of both species,  $T$  is the fraction of molecules converted to the triplet state and  $\tau_0$  is the characteristic time for the transition ( $\tau_0^{-1}$  is the transition rate),  $S$  is the ratio of half-axes ( $S = \omega_2/\omega_1$ ) and the irradiated volume  $V = 2\pi\omega_1^2\omega_2$ . Diffusion coefficient of the  $i$ -th component,  $D_i$ , may be calculated as  $D_i = \omega_1^2/4\tau_i$  and the hydrodynamic radius can be recalculated using the Stokes–Einstein formula,  $R_H = kT/(6\pi D\eta)$ , where  $k$  is the Boltzmann constant,  $T$  temperature and  $\eta$  viscosity of the solvent.

**Static light scattering (SLS).** Measurements were performed on a Sofica instrument equipped with a He-Ne laser. Data were treated by the standard Zimm method<sup>11</sup>. Refractive index increments,  $dn/dc$ , were measured on a Brice–Phoenix differential refractometer.

*Dynamic light scattering (DLS).* An ALV 5000 multibit, multitaup autocorrelator (Langen, Germany) and an He-Ne laser ( $\lambda = 633$  nm) were employed. The solutions for measurements were filtered through  $0.2 \mu\text{m}$  Acrodisc filters. Measurements were performed with solutions of the lowest possible concentration (*ca*  $0.1 \text{ g l}^{-1}$ ) at different angles and temperature of  $25^\circ\text{C}$ . Analysis of the data was performed by fitting the experimentally measured  $g_2(t)$ , the normalized intensity autocorrelation function, which is related to the electric-field correlation function,  $g_1(t)$ , by the Siegert relation<sup>12</sup>

$$g_2(t) - 1 = \beta |g_1(t)|^2, \quad (4)$$

where  $\beta$  is a factor accounting for deviation from ideal correlation.

The average diffusion coefficient and polydispersity was evaluated using the cumulant method, which employs the relation<sup>12</sup>

$$g_1(t) = \exp[-\Gamma(q)t + \mu_2(q)t^2 + \Theta(t)^3]. \quad (5)$$

The average diffusion coefficient may be obtained from the first term as  $D = \Gamma/q^2$ , and the polydispersity index of the diffusion coefficient distribution,  $P_D$ , from the second moment of the correlation curve,  $P_D = \mu_2(q)/\Gamma(q)^2$ . Here  $q = (4\pi n_0/\lambda) \sin(\theta/2)$  is the magnitude of the scattering vector,  $\Gamma = 1/\tau$  is the relaxation rate,  $\theta$  the scattering angle,  $n_0$  the refractive index of pure solvent and  $\lambda$  the wavelength of the incident light. The term  $\Theta(t^3)$  is a small error of the order  $t^3$ . The hydrodynamic radius  $R_H$  was evaluated from the diffusion coefficient using the Stokes–Einstein formula.

*Atomic force microscopy (AFM).* All measurements were performed in the tapping mode under ambient conditions using a commercial scanning probe microscope, Digital Instruments NanoScope dimensions 3, equipped with a Nanosensors silicon cantilever, typical spring constant  $40 \text{ N m}^{-1}$ . Polymeric micelles were deposited on a fresh (*i.e.*, freshly peeled off) mica surface (flogopite, theoretical formula  $\text{KMg}_3\text{AlSi}_3\text{O}_{10}(\text{OH})_2$ , Geological Collection of the Charles University in Prague, Czech Republic) by a fast dip coating in a dilute micelle solution in pure water (copolymer concentration,  $C_p$ , *ca*  $2 \times 10^{-2} \text{ g l}^{-1}$ ). After the evaporation of water, the samples for AFM were dried in a vacuum oven at ambient temperature for *ca* 5 h.

*UV-VIS absorption spectroscopy and fluorometry.* Both techniques are described in the accompanying paper<sup>13</sup>.

## RESULTS AND DISCUSSION

### *Light Scattering Characterization and the Study of the Aggregation of Micelles*

The micelles prepared in acid and alkaline media differ in molar mass and size, which is understandable because they form under different conditions. Since water is a very strong precipitant for PS, the obtained micelles are the kinetically frozen nanoparticles (with glassy PS cores). As far as the micelles in acid media are concerned, the insoluble PS block is short as compared with the total length of soluble blocks (PVPH<sup>+</sup> and PEO) and the association number (in the “critical mixture”, *i.e.*, the mixture in which the micelliza-

tion equilibrium freezes) is therefore lower than that in the alkaline solution where both PS and PVP blocks are insoluble. In contrast to our earlier studies of similar kinetically frozen micellar systems, we found that the mass and size of PS-PVP-PEO micelles depend also on the copolymer concentration during dialysis and on other preparation conditions. It should be mentioned that this dependence is quite pronounced in alkaline media.

The first two samples were prepared under the conditions when the final concentration after dialysis was *ca* 2 g l<sup>-1</sup> and the ionic strength was moderately high, *I* = 0.1. Their basic characterization was performed by light scattering since it is a currently used "benchmark" technique in our laboratory. In order to remove dust particles, the solutions were filtered very slowly and carefully to prevent the secondary aggregation of micelles. The molar mass (measured by static light scattering) and the hydrodynamic radius of micelles prepared in acid and alkaline media (measured by quasielastic light scattering) were:  $M_w = 2.7 \times 10^6$  g mol<sup>-1</sup> and  $R_H = 37$  nm and  $M_w = 5.4 \times 10^6$  g mol<sup>-1</sup> and  $R_H = 35$  nm, respectively.

We found that the compact middle PVP layer in onion micelles can be dissolved during dialysis against HCl without any changes in the micellar molar mass. (This means that the secondary aggregation may be, in principle, avoided.) We were able to reproduce molar masses after acidification, but not after alkalization. This phenomenon will be discussed later.

Since we observed that mechanical shear may produce changes in properties of micellar solutions, we performed the alkalimetric titration of acid solutions of micelles ( $M_w = 2.7 \times 10^6$  g mol<sup>-1</sup> and  $R_H = 37$  nm) under vigorous stirring. The transition at pH 4.8 was always accompanied by a strong deepening of opalescence, which was well visible with a naked eye. The light scattering measurement yields a very high value of molar mass and hydrodynamic radius of water dispersed particles,  $M_w = 36.0 \times 10^6$  g mol<sup>-1</sup> and  $R_H = 62$  nm. After the acidimetric back-titration to pH *ca* 2, the molar mass and hydrodynamic radius dropped to  $M_w = 4.8 \times 10^6$  g mol<sup>-1</sup> and  $R_H = 39$  nm. Later we found that changes in molar mass by a factor of up to 4 (depending on ionic strength) may be caused just by shaking an acid solution of micelles. A comparable shaking of an alkaline solution results in much more pronounced changes – by almost one order of magnitude. However, it is worth mentioning that micellar aggregates are stable in aqueous solutions and do not precipitate and the scattering intensity does not change, at least for the time period of several months.

What is interesting, it is the strong correlation of the secondary aggregation with the collapse and deprotonation of the PVP block. Although some aggregation may occur during vigorous stirring at a constant low pH, a re-

ally massive aggregation requires deprotonation of the PVP block. Figure 1 shows the intensity of the light scattered at  $90^\circ$  during the alkalimetric titration performed under intensive stirring. The curve shows a steep increase in the scattering intensity close to pH 4.8.

A systematic study of the aggregation process and factors that influence this phenomenon is in progress. The results obtained so far suggest that the aggregation is a result of a limited solubility of concentrated PEO chains in micellar shells. Because the cores of PS-PVP-PEO micelles are small, the local concentration of PEO segments is high close to the core. Since the PEO chains are fairly long in comparison with the mixed PBA-PVP/PVP-PEO systems that we studied earlier<sup>3e</sup>, the hydration of the inner shell is difficult. At first, we were tempted to assume that the secondary aggregation is a result of the partial crystallization of PEO blocks. The following arguments seemed to support this assumption: (i) The relatively high concentration of fairly long PEO chains in micellar shells promotes crystallization. (ii) The formation of crystalline domains and the loss of mobility of parts of PEO chains in the dense inner shell close to the PS core reduce the solubility of micelles and cause their aggregation. (iii) Upon a close approach of two or more micelles, local concentration of PEO blocks increases at micellar peripheries due to the interpenetration of PEO shells, which, in turn, may trigger additional crystallization of parts of chains from different micelles and result in a fairly strong intermicellar bridging. However,  $^1\text{H}$  NMR spectra do not detect any decrease in the mobility of  $-\text{CH}_2\text{O}-$  protons, nor a de-

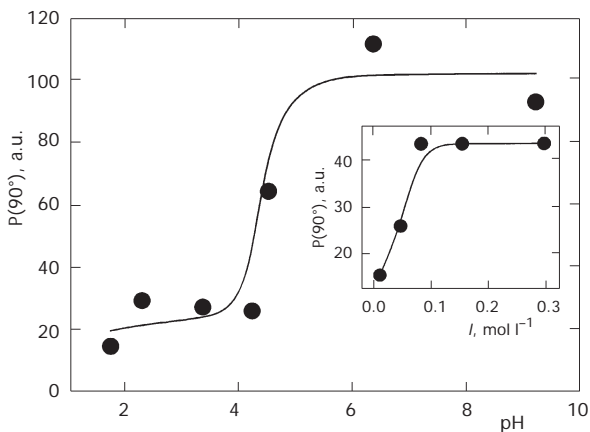


FIG. 1

Light scattering intensity,  $P(90^\circ)$ , of PS-PVP-PEO micelles, as a function of pH, measured during alkalimetric titration of an aqueous PS-PVP-PEO solution (polymer concentration,  $C_p = 2 \text{ g l}^{-1}$ ) in  $0.01 \text{ M}$  HCl with  $1 \text{ M}$  NaOH. Inset:  $P(90^\circ)$  as a function of the ionic strength  $I$



crease in the fraction of mobile  $-\text{CH}_2\text{O}-$  groups upon shaking the solution. Therefore, the PEO crystallization does not seem to be the driving force for the aggregation. We believe that the aggregation is a result of hindered hydration of PEO units, mainly due to the crowding of polymer segments in the dense inner shell around the core. In the dissolution and hydration of PEO chains, *ca* 6  $\text{H}_2\text{O}$  molecules<sup>14a</sup> are firmly bound to each PEO unit<sup>14a</sup>. Therefore the LCST of PEO in water is relatively low, around  $100\text{ }^\circ\text{C}$ <sup>14b</sup>. In the case of long and concentrated PEO blocks in micellar shells, the solvent entropy penalty is appreciable and therefore the solubility is fairly reduced<sup>14</sup>.

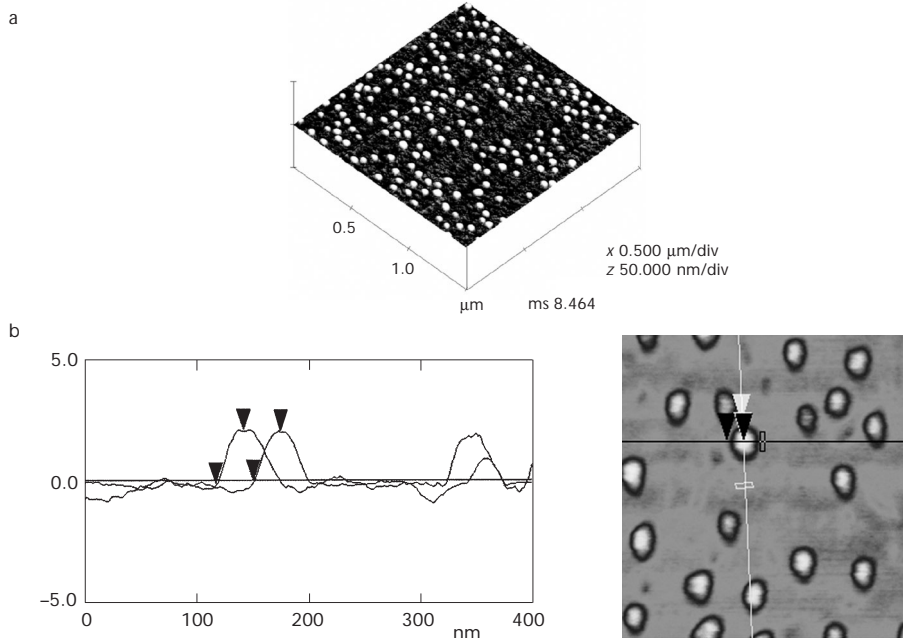
The neutral onion micelles show a considerably higher aggregation affinity than the core/shell micelles with partly charged PVP chains. This difference may be understood and rationalized by the following arguments. The decreased aggregation tendency in systems of protonated micelles is, for the most part, due to electrostatic repulsion between charged shells of different micelles. Since small ions screen the electrostatic repulsion, the aggregation depends strongly on their concentration and in acid solutions may be suppressed by increased ionic strength. Higher stability of acid core/shell micelles in comparison with alkaline onion micelles may be attributed to some extent to slight protonation of PEO chains and to energetically favorable hydration of protonated PEO segments in acid media.

The effect of ionic strength on the aggregation is shown in the insert in Fig. 1. The curve shows the scattering intensity measured from acid solutions as a function of increasing ionic strength. The experimental points were obtained as follows. The stock solution of micelles was divided into several portions. Different amounts of NaCl were added to raise the ionic strength. Then all solutions were shaken in a shaker for 1 min at a frequency of 10 Hz and treated in an ultrasonic bath for 10 s to remove air bubbles prior to scattering measurements. The scattering intensity was measured at the scattering angle  $90^\circ$  and plotted as a function of ionic strength  $I$ . At low  $I$ , the effect is only mild. The scattering increases steeply in the range of  $I$  *ca* 0.01–0.1 and levels off at  $I$  higher than 0.1.

Supplementary measurements, including differential scanning calorimetry and low-angle X-ray scattering are being prepared and results will be reported soon. So far, we have not obtained an ultimate proof that the observed complex behavior is not the result of the crystallization-based aggregation. However, all indirect data together with observations of the PEO solubility made by other authors<sup>14</sup> support strongly the assumption that the hindered hydration of PEO segments in dense inner shells of micelles results in the reduced solubility and stability of micelles, which causes their aggregation.

*Atomic Force Microscopy*

Micelles in both acid and alkaline media were studied by AFM (using the soft tapping mode) after deposition on the fresh mica (flogopite type) surface by fast dip coating. For a successful AFM study, the solution must not contain any salt that might crystallize on the surface and bury the nanoparticles of interest. Therefore we prepared new samples of micelles in pure water and in acid solution of hydrochloric acid. Figure 2a shows a large  $1.5 \mu\text{m} \times 1.5 \mu\text{m}$  scan of onion micelles deposited on the surface from a very dilute neutral solution in pure water (copolymer concentration,  $C_p$ , *ca*  $2 \times 10^{-2} \text{ g l}^{-1}$ ). The micelles were prepared in pure water (final pH *ca* 6, final concentration  $2 \text{ g l}^{-1}$ ). A tilted scan shows fairly uniform spherical nanoparticles. The size is smaller than that of micelles prepared in salt solutions which we studied by QELS and SLS. Nevertheless, it compares quite well with their size measured by FCS (see the section analysis and the zoomed-in scan below) and it is also consistent with the  $M_n$  evaluated independently by FCS. As far as the size and shape of micelles observed by AFM

**FIG. 2**

a AFM scan ( $1.5 \mu\text{m} \times 1.5 \mu\text{m}$ ) of PS-PVP-PEO micelles deposited on the mica surface from a dilute solution (polymer concentration,  $C_p = 2 \times 10^{-2} \text{ g l}^{-1}$ ) in pure water, pH *ca* 6. b Section analysis of the micelles

are concerned, some precaution is needed. It is necessary to keep in mind that the shape of surface-deposited micelles differs from those in solution. The PS cores in simple core/shell micelles and the PS cores covered by a collapsed PVP layer in onion micelles are quite rigid and should not appreciably deform, either after deposition on the surface or in contact with the AFM tip, since both copolymers are glassy at ambient temperatures. The soluble blocks spread on the hydrophilic mica surface and are fairly stretched. The stretching is due, in part, to favorable interactions of PEO with mica and to the entropy effect. Since the maximum vertical distances are *ca* 3 nm, while the horizontal distances are *ca* 60 nm, the deposition may be regarded as the transition from a 3D to 2D space. In analogy with the behavior of 2D and 3D star polymers, we may expect a non-negligible stretching of shell-forming blocks at the surface. Such stretching was predicted by scaling theories not only for the stars, but for all types of chains. Flory<sup>15a</sup> and later Fisher<sup>15b,15c</sup> showed that the average end-to-end distance of a single self-avoiding chain,  $R$ , scales (in systems differing in dimensionality  $d$ ) with  $R \propto N^{3/(d+2)}$ . Eisenberg *et al.* proved a significant stretching of micelles deposited at surfaces and flat interfaces experimentally<sup>15d</sup>. Recently we studied polystyrene-*block*-poly(methacrylic acid) micelles with glassy PS cores by small-angle neutron scattering (SANS)<sup>3i</sup> and by AFM<sup>3m</sup>. In the case of fairly large PS-PMA micelles, the 20 nm diameter of the PS core obtained by SANS compares nicely with the maximum vertical distances, which were estimated to be slightly above 20 nm. However, only fairly large cores, in which the conformations of the core-forming PS blocks are not too restricted, are really rigid. The conformations of chains confined in small volumes differ from those in bulk polymers and the mobility of chains increases. Kajiyama *et al.* studied the glass transition temperature and chain mobility in thin polystyrene and poly(methyl methacrylate) films and found that the chain mobility in thin films is higher than that in bulk polymers and that the glass transition temperature decreases with decreasing thickness of the film<sup>15e</sup>. Similar results were also obtained by other authors<sup>15f</sup>. All experimental data suggest that the association number is very low and the cores are small. Hence the cores do not have to be necessarily rigid and we cannot rule out some deformation of the PS core. The section analysis of the zoomed-in part of the scan (Fig. 2b) shows that the micelles on the surface resemble pancakes. The maximum horizontal distances are only *ca* 3 nm which indicates that the PS cores of micelles are fairly small (appreciably smaller than the cores of mixed onion micelles<sup>3e</sup>). The observed value leads to a very low association number of several chains only. If we admit a small

deformation of the core and assume that the non-deformed core radius,  $R_C$ , could be *ca* 2–2.5 nm, we get an association number of few tens, which agrees well with FCS results. Figure 3a shows a 500 nm  $\times$  500 nm scan of micelles deposited from a slightly more concentrated neutral solution (1.5 times higher concentration as compared with the previous picture). Besides the uniformity in sizes of spherical micelles observed in both figures, the tendency to aggregate at higher concentration is quite obvious. Despite the fact that the surface is only partly covered by micelles, the formation of chains and clusters of micelles is well apparent. Figure 3b shows micelles deposited from an acid solution. These micelles were prepared in the form of onions (shown in the previous figure in the neutral solution) and transferred into the acid (0.01 M HCl) solution, which caused protonation and swelling of PVP blocks and the transition of onion micelles to the state of core/shell micelles. It is evident that the size of core/shell micelles is fairly similar to the parent onion micelles. The image is much less sharp and the tilted view of the surface shows micelles as ellipsoids partly oriented in the direction of the scan. The worse resolution and the apparent ellipsoidal shape are side effects of the AFM scanning. The PS-PVP-PEO micelles do not stick strongly to the surface. We found, by applying the minimum force contact mode (*ca* 40 N m<sup>-1</sup>) that micelles are quantitatively removed from the surface and an atomically flat mica surface is observed. For a successful study of polymeric micelles, the tapping mode only may be applied. However, the silicon nitride probing tip is slightly negatively charged both in aqueous solutions and in moist media<sup>16a</sup> and it interacts with the positively charged PVPH<sup>+</sup> blocks of micelles. Therefore, even in the soft tapping mode, the electrostatic interaction of the tip with micelles produces an at-

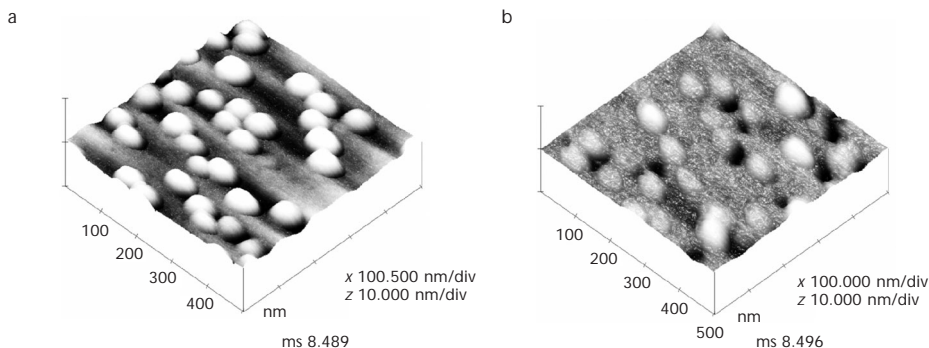


FIG. 3

AFM scan (500 nm  $\times$  500 nm) of PS-PVP-PEO micelles deposited on the mica surface from a dilute solution (polymer concentration,  $C_p = 3 \times 10^{-2}$  g l<sup>-1</sup>) in: a pure water (pH *ca* 6), b 0.01 M HCl

tractive force and may displace micelles slightly forth and back at the surface during the scanning. If this disturbance happens, the tip “feels the object longer” in the direction of the scan and the spherical object is imaged as an ellipsoid. Since the tip moves the micelles slightly and irregularly forth and back, the obtained image is not sharp. These effects were observed later by more advanced measurements<sup>16b</sup>.

Figure 4 shows an AFM scan of micellar aggregates deposited from the same solution as the well-resolved micelles shown in Fig. 2. The only difference in the sample preparation consisted in the vigorous stirring immediately before the deposition. In this case, we can see distinct micellar aggregates at some places (Fig. 4a), but no micelles at all in most parts, and the AFM scan shows only patches of polymeric film of very irregular thickness (Fig. 4b). Since the micellar aggregates seem to be stable in solution, we expect that a strong aggregation occurs on the surface after deposition of the sample. Section analysis of distinct micellar particles (Fig. 4c) compares fairly well with light scattering data.

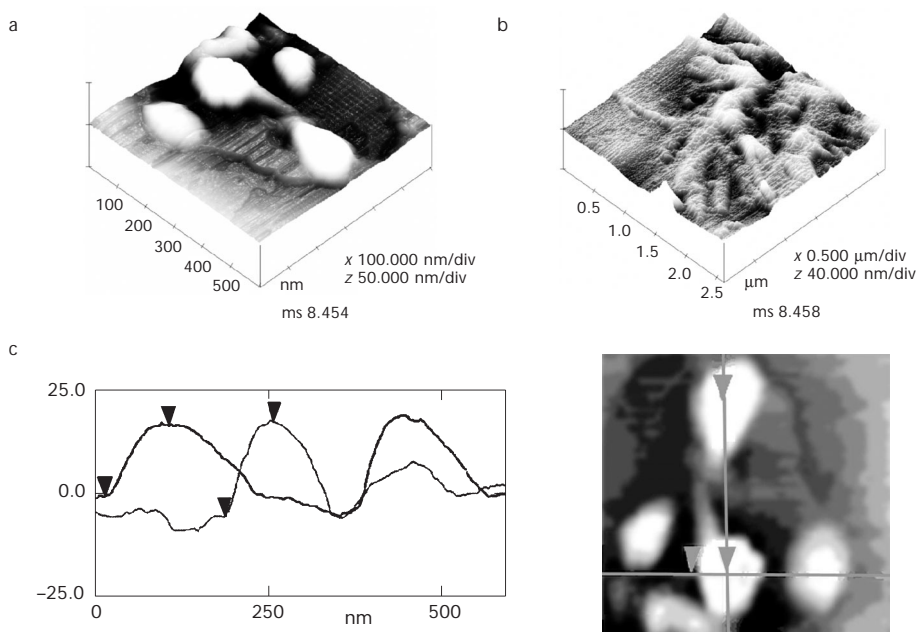


FIG. 4

AFM scan (500 nm  $\times$  500 nm) of PS-PVP-PEO micelles deposited on the mica surface from a dilute solution (polymer concentration,  $C_p = 3 \times 10^{-2} \text{ g l}^{-1}$ ) in pure water (pH ca 6) after vigorous stirring of the stock solution ( $C_p = 2 \text{ g l}^{-1}$ ). a Micellar aggregates, b PS-PVP-PEO film and c section analysis of micellar aggregates

### The Degree of PVP Protonation

In order to account for the already mentioned small changes in the size of micelles after protonating and swelling the middle PVPH<sup>+</sup> layer (observed both by QELS and AFM), we performed a careful potentiometric titration of micellar solutions aimed at the estimation of the fraction of protonated PVPH<sup>+</sup> units. We used the methodology described in our earlier paper<sup>3h</sup> and found that in 0.1 M HCl (after careful dialysis repeated many times), the fraction of protonated PVP is only *ca* 0.3. (This value is comparable with that for PS-PVP star copolymer micelles, which was *ca* 0.4 (ref.<sup>3h</sup>.) The electrostatic repulsion and PVP stretching are therefore quite small and the difference in sizes between the core/shell and onion micelles is also pretty small.

### Binding of ORB to Micelles

For a successful FCS study of ORB-labeled micelles, it is necessary to get information on the binding kinetics and the equilibrium ORB partition between micelles and the aqueous solution. Further we have to know spectral properties of the micelle-bound ORB at different probe-to-micelle ratios. Figure 5 shows the UV-VIS absorption spectra at different times after mixing an ORB solution with a solution of onion micelles for the probe-to-

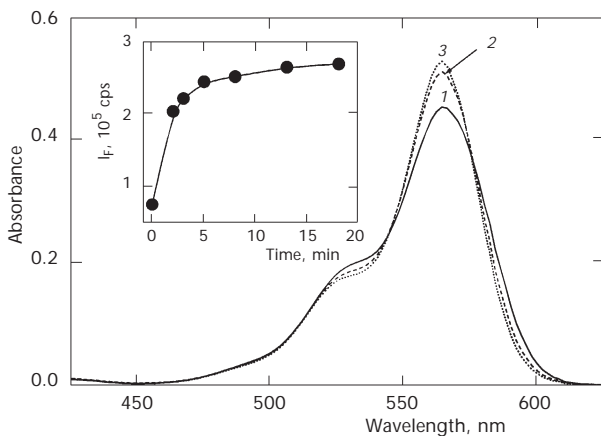


FIG. 5

Absorption spectra of ORB (probe concentration,  $c_F = 5 \mu\text{mol l}^{-1}$ ) added to PS-PVP-PEO micelles in 0.01 M HCl (polymer concentration,  $C_p = 2 \times 10^{-2} \text{ g l}^{-1}$ ) immediately after addition (curve 1), 2 min after addition (curve 2) and 20 min after addition (curve 3) to the micelles. Inset: ORB fluorescence intensity,  $I_F$  (excitation at 564 nm, emission at 585 nm) as a function of time after addition to the micelles

micelle ratio *ca* 5, in an acid solution (0.01 M HCl). Immediately upon mixing, the water-dissolved ORB exists in the associated form. Hence the spectrum consists of spectra of the monomer, J- and H-dimers and higher aggregates<sup>17a,17b</sup>. Since the probe-to-micelle ratio is low, individual probes bind at the compact middle layer/shell interface (after penetration into the shell) as monomers and the spectrum changes in favor of the monomer spectrum. In the insert, the fluorescence intensity during the binding is depicted as a function of time. After excitation, the fluorescence is self-quenched due to the presence of H-aggregates which are not only non-fluorescent, but act as efficient energy traps<sup>17c</sup>. The fluorescence intensity increases with time and levels-off at long times, *ca* 20 min.

### *Fluorescence Correlation Spectroscopy Study*

Fluorescence correlation spectroscopy was used for the measurement of the number-average molar masses of micelles,  $M_n$  and the number-average-based hydrodynamic radii,  $(R_H)_n$ . It should be pointed out that the hydrodynamic radius is not strictly the number average, instead, it is based on the number-average diffusion coefficient. The measurement of  $M_n$  is straightforward, accurate and reliable. It does not require a measurement of the autocorrelation function of fluctuations and fitting of the autocorrelation decay to the theoretical expression. The precision of the determination depends only on the calibration accuracy, *i.e.*, on the accurate determination of the effective irradiated volume. The principle of the measurement is based on monitoring the average frequency of fluctuations. The fluctuations in the fluorescence intensity are caused by diffusion of particles in and out of the irradiated volume. Hence their average frequency is proportional to the number of fluorescent particles in the active volume,  $N$ . The measurement of  $M_n$  can be briefly outlined as follows. The micellar solution is slowly titrated by a solution containing fluorescent probes that bind strongly to micelles and the average frequency of fluctuations is measured as a function of the probe concentration,  $c_F$  (after equilibration, which may take sometimes hours). At  $c_F$  lower than the concentration of micelles,  $c_{mic}$ , individual probes bind to different micelles and the number of fluorescent species in the active volume (and the frequency of fluctuations) increases. When all micelles are labeled by at least one probe, more probes start to bind to the same micelles. The fluctuations become larger, but their frequency is constant because the number of fluorescent species does not change any longer. The aforementioned simplified description should lead to experimental curves consisting of two straight lines: (i) a lin-

early rising first part for  $c_F$  up to  $c_{mic}$  and (ii) a constant part for higher  $c_F$ . The leveling-off part of the curve yields the number of the fluorescent species, *i.e.*, the number of micelles in the active volume. The knowledge of the number of micelles, active volume and polymer concentration allows for the calculation of the number-average molar mass of micelles. The experimentally measured curves are smooth and their shape is sometimes quite complex as a consequence of the Poisson distribution of probes among micelles and other effects. We have shown in our recent papers that the limiting part of the curve for high  $c_F$  always provides correct values of  $M_n$  (not only for any distribution of probes among micelles, but also for systems in which impurity quenching cannot be ruled out, *etc.*)<sup>3m</sup>.

TABLE II

Aggregation number,  $n$ , molar mass,  $M_n$ , and hydrodynamic radius,  $R_H$ , of PS-PVP-PEO micelles: core/shell micelles (a), core/shell micelles from onions (b), onion micelles (c) and onion micelles from core/shell micelles (d)

Micelle type	$n$	$M_n \times 10^{-6}$ , g mol <sup>-1</sup>	$R_H$ , nm
a	7.3	0.45	28.0
b	19.0	1.17	36.8
c	18.3	1.12	21.6
d	12.0	0.74	22.2

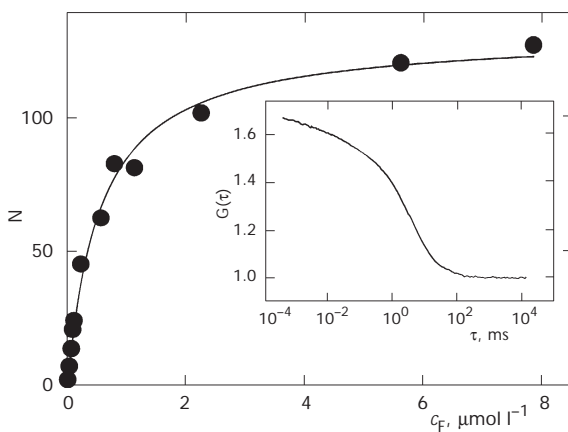


FIG. 6

ORB particle number,  $N$ , as a function of ORB concentration,  $c_F$ , of the ORB/PS-PVP-PEO system in 0.01 M HCl. Insert: Typical correlation curve for an FCS measurement of the ORB/PS-PVP-PEO system in 0.01 M HCl



Figure 6 shows a typical  $N$  vs  $c_f$  curve obtained for PS-PVP-PEO micelles in 0.01 M HCl. The curve is only little affected by impurity quenching at low  $c_f$  and the fairly long constant part allows for reliable evaluation of the molar mass, yielding a value of  $M_n = 4.5 \times 10^5$ . Molar masses of micelles prepared in 0.01 M HCl and 0.01 M NaOH and of those transferred from HCl to NaOH (and *vice versa*) are given in Table II. They prove without any doubt that the addition of an acid to onion micelles results in the dissolution of the middle PVP layer without changes in the molar mass. On the other hand, even the most careful conversion of core/shell micelles to onion micelles by alkalization is accompanied by aggregation and the molar mass of converted onions is higher than that of parent core/shell micelles.

The number-average-based hydrodynamic radii of micelles measured by FCS are also listed in Table II. A typical fluorescence fluctuation correlation curve for PS-PVP-PEO micelles prepared in 0.01 M HCl is shown in the insert in Fig. 6. The results show that the  $R_H$  of micelles prepared carefully (without any shaking or filtration) increases after the conversion of onion micelles to core/shell micelles due to partial stretching of charged PVPH<sup>+</sup> blocks. The observed change in size of micelles agrees with our earlier results on mixed micelles<sup>3e,3h</sup>.

To summarize the FCS study of PS-PVP-PEO micelles with ORB as a micelle-specific fluorescent tag, we found that (i) FCS is a suitable experimental technique which will certainly find a number of applications in polymer science and (ii) ORB is an excellent probe for the sorption-based tagging of amphiphilic polymeric nanoparticles.

## CONCLUSIONS

In this study, we have proved that triblock copolymer polystyrene-*block*-poly(2-vinylpyridine)-*block*-poly(ethylene oxide) forms two types of spherical nanoparticles in aqueous media depending on pH. The core/shell micelles with insoluble PS cores and soluble shells composed of diblocks of poly(2-vinylpyridine(partly protonated))-*block*-poly(ethylene oxide) exist at pH < 4.8, while at higher pH, the deprotonated PVP collapses and the three-layer onion micelles form. The onion micelle has a compact PS core covered by a collapsed PVP layer and a soluble PEO shell. Since water is a very strong precipitant for PS, both types of micelles have kinetically frozen cores.

Acidification leads to a fully reversible transition of one type of micelles into the other (accompanied by protonation and swelling/deprotonation and collapse of the middle PVP layer) without any changes in molar mass

of micelles. The observed changes in size comparable to systems of mixed onion micelles were studied earlier<sup>3e,3h</sup>.

The studied PS-PVP-PEO micelles show a strong tendency to aggregate. The aggregation may be provoked by stirring or shaking the solution. All indirect data suggest that the aggregation is a result of a decreased solubility of concentrated PEO chains in micellar shells. The core/shell micelles with PVPH<sup>+</sup> blocks are less apt to the aggregation than the neutral onion micelles because of the electrostatic repulsion between charged PVPH<sup>+</sup> blocks and a more convenient hydration of slightly protonated PEO chains.

From the methodological point of view, the study proves that octadecyl-rhodamine B is an excellent fluorescent probe for labeling water-soluble polymeric nanoparticles and that the fluorescence correlation spectroscopy is a suitable experimental technique for characterization of micelles and for studying the solution behavior of amphiphilic nanoparticles.

*This study was supported by the Grant Agency of the Czech Republic (grants No. 203/01/0536, No. 203/01/0735 and No. 203/02/D048) and by the Grant Agency of the Charles University (grant No. 215/2000/BCh/Pr). J. Humpolíčková and M. Hof would like to acknowledge support from the Ministry of Education, Youth and Sports of the Czech Republic (LN00A032).*

## REFERENCES

1. Webber S. E., Munk P., Tuzar Z. (Eds): *Solvents and Self-Organization of Polymers*. NATO ASI Ser. E, p. 327, 1996.
2. Hamley I. W.: *Physics of Block Copolymers*. Oxford University Press, Oxford 1998.
3. a) Kiserow D., Procházka K., Ramireddy C., Tuzar Z., Munk P., Webber S. E.: *Macromolecules* **1992**, *25*, 461; b) Ramireddy C., Tuzar Z., Procházka K., Webber S. E., Munk P.: *Macromolecules* **1992**, *25*, 2541; c) Tian M., Quin A., Ramireddy C., Webber S. E., Munk P., Tuzar Z., Procházka K.: *Langmuir* **1993**, *9*, 1741; d) Procházka K., Martin T. J., Munk P., Webber S. E.: *Macromolecules* **1996**, *29*, 6518; e) Procházka K., Martin T. J., Webber S. E., Munk P.: *Macromolecules* **1996**, *29*, 6526; f) Štěpánek M., Procházka K.: *Langmuir* **1999**, *15*, 8800; g) Štěpánek M., Procházka K., Brown W.: *Langmuir* **2000**, *16*, 2502; h) Tsililianis C., Voulgaris D., Štěpánek M., Podhájecká K., Procházka K., Tuzar Z., Brown W.: *Langmuir* **2000**, *16*, 6868; i) Pleštil J., Kříž J., Tuzar Z., Procházka K., Melnichenko Yu. B., Wignall G. D., Talingting M. R., Munk P., Webber S. E.: *Macromol. Chem. Phys.* **2001**, *202*, 553; j) Štěpánek M., Podhájecká K., Tesařová E., Procházka K., Tuzar Z., Brown W.: *Langmuir* **2001**, *17*, 4240; k) Podhájecká K., Štěpánek M., Procházka K., Brown W.: *Langmuir* **2001**, *17*, 4245; l) Matějčík P., Uhlík F., Limpouchová Z., Procházka K., Tuzar Z., Webber S. E.: *Macromolecules* **2002**, *35*, 9487; m) Matějčík P., Humpolíčková J., Procházka K., Tuzar Z., Špírková M., Hof M., Webber S. E.: *J. Phys. Chem. B* **2003**, *107*, 8232.
4. a) Viduna D., Limpouchová Z., Procházka K.: *Macromolecules* **1997**, *30*, 7263; b) Limpouchová Z., Viduna D., Procházka K.: *Macromolecules* **1997**, *30*, 8027; c) Jelínek K.,

- Limpouchová Z., Procházka K.: *Macromol. Theory Simul.* **2000**, *9*, 703; d) Uhlík F., Limpouchová Z., Matějčík P., Procházka K., Tuzar Z., Webber S. E.: *Macromolecules* **2002**, *35*, 9497.
5. a) Allen R. C., Mandelkern L.: *Polym. Bull.* **1987**, *17*, 473; b) Hager S. L., Macrury T. B.: *J. Appl. Polym. Sci.* **1980**, *25*, 1559; c) Ding N., Amis E. J.: *Macromolecules* **1991**, *24*, 3906.
6. a) Magde D., Elson E. L., Webb W. W.: *Phys. Rev. Lett.* **1972**, *29*, 705; b) Elson E. L., Magde D.: *Biopolymers* **1974**, *13*, 1; c) Magde D., Elson E. L., Webb W. W.: *Biopolymers* **1974**, *13*, 29.
7. a) Bastiaens P. I. H., Pap E. H. W., Widengren J., Rigler R., Visser A. J. W. G.: *J. Fluoresc.* **1994**, *4*, 377; b) Koralach J., Schwille P., Webb W. W., Feigenson G. W.: *Proc. Natl. Acad. Sci. U.S.A.* **1999**, *96*, 8461; c) Schwille P., Haupts U., Maiti S., Webb W. W.: *Biophys. J.* **1999**, *77*, 2251; d) Král T., Langner M., Beneš M., Baczynska D., Ugorski M., Hof M.: *Biophys. Chem.* **2002**, *95*, 135; e) Král T., Hof M., Langner M.: *Biol. Chem.* **2002**, 383, 331; f) Beneš M., Billy D., Hermens W. T., Hof M.: *Biol. Chem.* **2002**, 383, 337.
8. a) Erhardt R., Boker A., Zettl H., Kaya H., Pyckhout-Hintzen W., Krausch G., Abetz V., Mueller A. H. E.: *Macromolecules* **2001**, *34*, 1069; b) Zhao J. J., Bae S. C., Xie F., Granick S.: *Macromolecules* **2001**, *34*, 3123.
9. Thompson N. L. in: *Topics in Fluorescence Spectroscopy* (J. R. Lakowicz, Ed.), Vol. 5. Plenum Press, New York 1991.
10. a) Webb W. E. in: *Fluorescence Correlation Spectroscopy. Theory and Applications* (R. Riedler and E. S. Elson, Eds). Springer-Verlag, Berlin 2001; b) Hink M. A., van Hoek A., Visser A. J. W. G.: *Langmuir* **1999**, *15*, 992; c) Koppel D. E.: *Phys. Rev.* **1974**, *10*, 1938; d) Kask P., Günter R., Axhausen P.: *Eur. Biophys. J.* **1997**, *25*, 163; e) Meseth U., Wohland T., Rigler R., Vogel H.: *Biophys. J.* **1999**, *76*, 1619; f) Edman L.: *J. Phys. Chem. A* **2000**, *104*, 6165; g) Wohland T., Rigler R., Vogel H.: *Biophys. J.* **2001**, *80*, 2987.
11. Kratochvíl P.: *Classical Light Scattering in Polymer Solutions*. Elsevier, Amsterdam 1987.
12. Chu B.: *Laser Light Scattering*, 2nd ed. Academic Press, New York 1991.
13. Humpolíčková J., Procházka K., Hof M.: *Collect. Czech. Chem. Commun.* **2003**, *68*, 2105.
14. a) Bieze T. W. N., Barnes A. C., Huige C. J. M., Enderby J. E., Leyte J. C.: *J. Phys. Chem.* **1994**, *98*, 6568; b) Hammouda B., Ho D., Kline S.: *Macromolecules* **2002**, *25*, 8578; c) Polverari M., van de Ven T. G. M.: *J. Phys. Chem.* **1996**, *100*, 13687.
15. a) Flory P.: *Principles of Polymer Chemistry*, Chap. XII. Cornell University Press, Ithaca 1971; b) Fisher M.: *J. Phys. Soc. Jpn.* **1969**, *26(Suppl.)*, 44; c) de Gennes P. G.: *Scaling Concepts in Polymer Physics*, Chap. I. Cornell University Press, Ithaca 1979; d) Zhu J. Y., Eisenberg A., Lennox R. B.: *J. Am. Chem. Soc.* **1991**, *113*, 5583; e) Kajiyama T., Tanaka K., Takahara A.: *Macromolecules* **1995**, *28*, 3482; f) Jean Y. C., Zhang R. W., Cao H., Yuan J. P., Huang C. M., Nielsen B., Asoka-Kumar P.: *Phys. Rev. B: Condens. Matter* **1997**, *56*, R8459.
16. a) Johnson C. A.: *Digital Instrum. Rep.* **1997**, *7*, AN09; b) Johnson C. A., Lenhoff A. M.: *J. Colloid Interface Sci.* **1996**, *179*, 587.
17. a) Fujii T., Nishikiori H., Tamura T.: *Chem. Phys. Lett.* **1995**, *233*, 424; b) del Monte F., Mackenzie J. D., Levy D.: *Langmuir* **2000**, *16*, 7377; c) MacDonald R. I.: *J. Biol. Chem.* **1990**, *265*, 13533.